JOC Article

Synthesis, Structure, and Transannular $\pi-\pi$ Interaction of Three- and Four-Layered [3.3]Paracyclophanes[1]

Masahiko Shibahara,*[,†] Motonori Watanabe,[‡,§] Tetsuo Iwanaga,[||] Taisuke Matsumoto,[‡] Keiko Ideta,[‡] and Teruo Shinmyozu[‡]

Department of Chemistry, Faculty of Education and Welfare Science, Oita University, 700 Dannoharu, Oita 870-1192, Japan, Institute for Materials Chemistry and Engineering (IMCE) and Department of Molecular Chemistry, Graduate School of Sciences, Kyushu University, 6-10-1 Hakozaki, Fukuoka 812-8581, Japan, and Department of Chemistry, Faculty of Science, Okayama University of Science, 1-1 Ridaicho, Okayama 700-0005, Japan

Received February 8, 2008

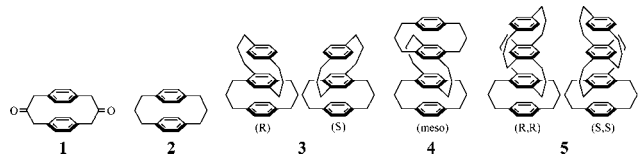

The synthesis of three- and four-layered [3.3]paracyclophanes ([3.3]PCPs) **3**−**5** has been accomplished by utilizing the (*p*-ethylbenzenesulfonyl)methyl isocyanide (EbsMIC) method. The structures of the three- to four-layered [3.3]PCPs **3**−**5** and their diones **8**, **10**, and **11** have been elucidated based on the ^{1}H NMR spectra and finally by X-ray structural analysis. In the three-layered [3.3]PCP-dione **8**, the trimethylene bridges of the [3.3]PCP unit assume a chair conformation similar to that of **2**, while the [3.3]PCP-2,11-dione unit assumes a boat conformation different from that of [3.3]PCP-dione **1** with a chair conformation. On the other hand, the two [3.3]PCP units in three-layered [3.3]PCP **3** both assume a boat conformation. In the four-layered [3.3]PCP-dione **10**, the two outer [3.3]PCP units assume a boat conformation while the inner dione unit has a chair conformation. The trimethylene bridges in the four-layered [3.3]PCP **4** are highly disordered even at −150 °C. All the outer benzene rings are distorted into a boat form while the inner ones are distorted into a twist form. In the electronic spectra, bathochromic shift and hyperchromic effect are observed, but the magnitude decreases with an increase in the number of layers and the spectra become structureless. In the charge-transfer (CT) bands of the three- to four-layered [3.3]PCPs **3**−**5** with tetracyanoethylene (TCNE), two absorption maxima (λ_{max}) are observed. The effect of an increase in the layers becomes significant, and the changes in the longest wavelength λ_{max} values from two to three and three to four are ca. 60 and 50 nm, respectively. By comparison of the stereoisomeric four-layered [3.3]PCPs **4** (meso) and **5** (racemic), the helical arrangement of the trimethylene bridges of **5** shows a more efficient transannular π-electronic interaction. In the three- to four-layered [3.3]PCP-diones, a magnitude of the CT interaction almost comparable to that of [3.3]PCP **2** was observed, and this indicates that the $-CH_2COCH_2-$ bridges inhibit the CT interaction and that this tendency is supported by the calculated HOMO energy levels and observed oxidation potentials. Three- and four-layered [3.3]PCPs **3**−**5** show reversible redox processes, and **4** and **5** show an electron-donating ability almost comparable to that of [3$_6$]CP. Very good correlation between the λ_{max} of the CT bands with TCNE and the oxidation potentials is observed.

1. Introduction

Multilayered cyclophanes (CPs) have served as suitable models for the study of their characteristic structural properties and transannular π-electronic interaction by choosing the appropriate cyclophane building blocks, i.e., para, meta, and metapara.[2–7] Since the first synthesis of various four-layered [2.2]PCP[8] and three-layered CPs,[9] several types of multilayered [2.2]CPs[4–6] were developed by Otsubo et al. and their characteristic chemical and physical properties have been reported.[10]

* To whom correspondence should be addressed. Phone: +81-97-554-7553. Fax: +81-97-554-7553. mshiba@cc.oita-u.ac.jp
† Oita University.
‡ IMCE, Kyushu University.
§ Department of Molecular Chemistry, Kyushu University.
|| Okayama University of Science.

(1) Multilayered [3.3]cyclophanes, part 3. For parts 1 and 2, see refs 2 and 3.
(2) Shibahara, M.; Watanabe, M.; Iwanaga, T.; Ideta, K.; Shinmyozu, T. *J. Org. Chem.* **2007**, *72*, 2865–2877.
(3) Muranaka, A.; Shibahara, M.; Watanabe, M.; Matsumoto, T.; Shinmyozu, T.; Kobayashi, N. To be submitted for publication.

10.1021/jo8003309 CCC: $40.75 © 2008 American Chemical Society
Published on Web 05/23/2008

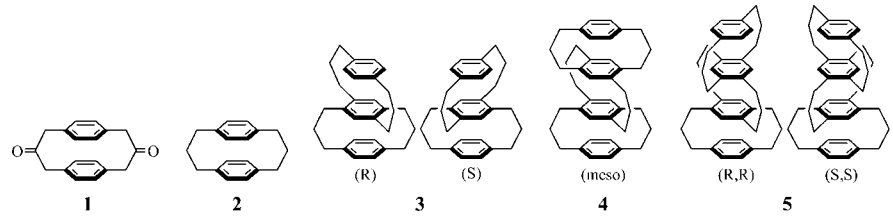

FIGURE 1. Multilayered [3.3]PCPs **2**−**5** and [3.3]PCP-dione **1**.

Among the various multilayered [2.2]CPs, paracyclophanes have chiroptical properties inherent in their helical features, and the synthesis of optically active multilayered [2.2]PCPs (up to six layers) was accomplished by Yamamoto et al.[7] Although [3.3]PCP is a better system than [2.2]PCP for investigation of electronic interaction because of the most appropriate transannular distance and much less strain of the benzene rings,[11] only a limited number of multilayered [3.3]CPs have been synthesized so far.[12–14] Otsubo et al. reported that three-layered [3.3][3.3]PCP showed the strongest electron-donating ability among the three-layered [*m.m*][*n.n*]PCPs (*m* and *n* = 2−4).[12] Mataka et al. reported the synthesis of up to four-layered [3.3]orthocyclophanes.[14b]

In the previous paper, we reported that the electron-donating ability of the multilayered [3.3]MCPs gradually increases with an increase in the layers, but the magnitude becomes less significant as the number of layers increases.[2] The moderate electron-donating ability of the multilayered [3.3]MCPs compared to that of the [3$_n$]CPs[15] may be ascribed to the tilted overlap of the benzene rings in the former. Quite interestingly, the anti geometry of the [3.3]MCP-2,11-dione moiety in the multilayered [3.3]MCPs serves as an electron insulator, and this suggested the importance of through-bond interaction for electronic interaction. Lately, our collaborators, Muranaka et al., reported the CD spectral properties and absolute configuration of *R*-(−)- and *S*-(+)-three-layered [3.3]PCPs **3** (Figure 1), and they concluded that the chiroptical properties of **3** are little affected by the conformation of the bridge carbon atoms, twisted structure, and deformation of the benzene rings.[3] This interpretation is different from that for multilayered [2.2]PCP, where distorted benzene rings are reported to be responsible for the CD spectra.[7b]

A systematic study on the multilayered [3.3]PCPs may provide (1) general synthetic methods for multilayered [3.3]PCPs, (2) further information on the electronic interaction through completely stacked and less strained benzene rings with appropriate distances, and (3) absolute configuration and chiroptical properties. We wish to report here the synthesis, structure, and electronic interaction of the three- and four-layered [3.3]PCPs **3**−**5** along with their synthetic intermediate diones **8**, **10**, and **11**.

2. Results and Discussion

Synthesis. In the previous paper, we already reported the synthesis of three-layered [3.3]PCPs **3**.[3] We used (*p*-ethylbenzenesulfonyl)methyl isocyanide (EbsMIC)[16] instead of conventional (*p*-tolylsulfonyl)methyl isocyanide (TosMIC)[16c] for improvement of the solubility in CH_2Cl_2 in the critical coupling reaction.[17] The synthetic key intermediates in the synthesis of multilayered [3.3]PCPs are two-layered bis(bromomethyl) compound **6** (racemic)[3] and its EbsMIC adduct **9** (racemic). The two-layered bromide **6** was coupled with the EbsMIC adduct **7** to give three-layered dione **8** (racemic, 22%, Scheme 1). The Wolff−Kishner reduction of **8** afforded the three-layered [3.3]PCP **3** (racemic, 82%),[3,12] whose resolution was attained by HPLC separation with a chiral stationary phase (Daicel Chemical Industries, Ltd.: Chiralcel OD with 2-propanol).[3]

A similar coupling of the dibromide **6** (racemic) with its EbsMIC adduct **9** (racemic) provided the two-isomeric mixture of **10** (C_{2h}, meso) and **11** (D_2, racemic) with the ratio of 1.0:1.4 (**10**:**11**) based on the ^{1}H NMR integral ratio (Figure S1, Supporting Information). The separation of the meso and racemic isomers was accomplished by the difference in the solubility in acetonitrile: the less soluble isomer was meso **10** and the readily soluble one was a racemic mixture **11**. After silica gel column chromatography, pure **10** (meso) and **11**

(4) (a) Otsubo, T.; Mizogami, S.; Sakata, Y.; Misumi, S. *Tetrahedron Lett.* **1971**, *12*, 4803–4806. (b) Otsubo, T.; Mizogami, S.; Sakata, Y.; Misumi, S. *Tetrahedron Lett.* **1973**, *14*, 2457–2460. (c) Otsubo, T.; Mizogami, S.; Sakata, Y.; Misumi, S. *Tetrahedron Lett.* **1972**, *13*, 2927–2930. (d) Otsubo, T.; Mizogami, S.; Otsubo, I.; Tozuka, Z.; Sakagami, A.; Sakata, Y.; Misumi, S. *Bull. Chem. Soc. Jpn.* **1973**, *46*, 3519–3530.

(5) (a) Kannen, N.; Umemoto, T.; Otsubo, T.; Misumi, S. *Tetrahedron Lett.* **1973**, *14*, 4537–4540. (b) Kannen, N.; Otsubo, T.; Sakata, Y.; Misumi, S. *Bull. Chem. Soc. Jpn.* **1976**, *49*, 3307–3313. (c) Kannen, N.; Otsubo, T.; Sakata, Y.; Misumi, S. *Bull. Chem. Soc. Jpn.* **1976**, *49*, 3203–3207. (d) Kannen, N.; Otsubo, T.; Sakata, Y.; Misumi, S. *Bull. Chem. Soc. Jpn.* **1976**, *49*, 3208–3212.

(6) (a) Umemoto, T.; Otsubo, T.; Sakata, Y.; Misumi, S. *Tetrahydron Lett.* **1973**, *14*, 593–596. (b) Umemoto, T.; Otsubo, T.; Misumi, S. *Tetrahydron Lett.* **1974**, *15*, 1573–1676.

(7) (a) Nakazaki, M.; Yamamoto, K.; Tanaka, S. *J. Chem. Soc., Chem. Commun.* **1972**, 433. (b) Nakazaki, M.; Yamamoto, K.; Tanaka, S.; Kametani, H. *J. Org. Chem.* **1977**, *42*, 287–291.

(8) (a) Longone, D. T.; Chow, H. S. *J. Am. Chem. Soc.* **1964**, *86*, 3898–3899. (b) Longone, D. T.; Chow, H. S. *J. Am. Chem. Soc.* **1970**, *92*, 994–998.

(9) Hubert, A. J. *J. Chem. Soc. C.* **1967**, 13–14.

(10) For reviews, see:(a) Misumi, S.; Otsubo, T. *Acc. Chem. Res.* **1978**, *11*, 251–256. (b) Misumi, S. *Mem. Inst. Sci. Ind. Res., Osaka Univ.* **1976**, *33*, 53–71. (c) Misumi, S. In *Cyclophanes II*; Keehn, P. M., Rosenfeld, S. M., Eds.; Academic Press: New York, 1983: pp 573−624. (d) Vögtle, F. *Cyclophan-Chemie*; B. G. Teubner: Stuttgart, Germany, 1990.

(11) (a) Cram, D. J.; Bauer, R. H. *J. Am. Chem. Soc.* **1959**, *81*, 5971–5977. (b) Sheehan, M.; Cram, D. J. *J. Am. Chem. Soc.* **1969**, *91*, 3553–3558.

(12) (a) Otsubo, T.; Kohda, T.; Misumi, S. *Tetrahedron Lett.* **1978**, *19*, 2507–2510. (b) Otsubo, T.; Kohda, T.; Misumi, S. *Bull. Chem. Soc. Jpn.* **1980**, *53*, 512–517.

(13) Breidenbach, S.; Ohren, S.; Nieger, M.; Vögtle, F. The proceeding of the 8th International Symposium on Novel Artomatic Compounds (ISNA-8), Braunschweike, Germany, July−August, 1995. But no report on the synthesis of three-layered [3.3]MCP has been published yet.

(14) (a) Mataka, S.; Mitoma, Y.; Thiemann, T.; Sawada, T.; Taniguchi, M.; Kobuchi, M.; Tashiro, M. *Tetrahedron* **1997**, *53*, 3015–3026. (b) Mataka, S.; Shigaki, K.; Sawada, T.; Mitoma, Y.; Taniguchi, M.; Thieman Thies.; Ohga, K.; Egashira, N. *Angew. Chem., Int. Ed.* **1998**, *37*, 2532–2534.

(15) (a) Sakamoto, Y.; Miyoshi, N.; Shinmyozu, T. *Angew. Chem., Int. Ed. Engl.* **1996**, *35*, 549–550. (b) Sakamoto, Y.; Miyoshi, N.; Hirakida, M.; Kusumoto, S.; Kawase, H.; Rudzinski, J. M.; Shinmyozu, T. *J. Am. Chem. Soc.* **1996**, *118*, 12267–12275. (c) Sakamoto, Y.; Shinmyozu, T. *Recent Res. Dev. Pure Appl. Chem.* **1998**, *2*, 372–399.

(16) EbsMIC 11 was synthesized by modified procedures starting from ethylbenzene: (a) Clarke, H. T.; Babcook, G. S.; Murray, T. F. *Organic Syntheses*, 2nd ed.; Wiley: New York, 1967; Collect. Vol. I, pp 85−87. (b) Field, L.; Clark, R. D. *Organic Syntheses*; Wiley: New York, 1963; Collect. Vol. IV, pp 674−677. (c) Hoogenboom, B. E.; Oldenziel, O. H.; van Leusen, A. M. *Organic Syntheses*; Wiley: New York, 1988; Collect. Vol. VI, pp 987−990.

(17) (a) Possel, O.; van Leusen, A. M. *Tetrahedron Lett.* **1977**, *18*, 4229–4232. (b) Kurosawa, K.; Suenaga, M.; Inazu, T.; Yoshino, T. *Tetrahedron Lett.* **1982**, *23*, 5335–5338. (c) Shinmyozu, T.; Hirai, Y.; Inazu, T. *J. Org. Chem.* **1986**, *51*, 1551–1555. (d) Sasaki, H.; Kitagawa, T. *Chem. Pharm. Bull.* **1983**, *31*, 2868–2878. (e) Breitenbach, J.; Vögtle, F. *Synthesis* **1992**, 41–42. (f) Sentou, W.; Satou, T.; Yasutake, M.; Lim, C.; Sakamoto, Y.; Itoh, T.; Shinmyozu, T. *Eur. J. Org. Chem.* **1999**, 1223–1231.

SCHEME 1. Synthetic Route to Three- and Four-Layered [3.3]PCPs 3−5

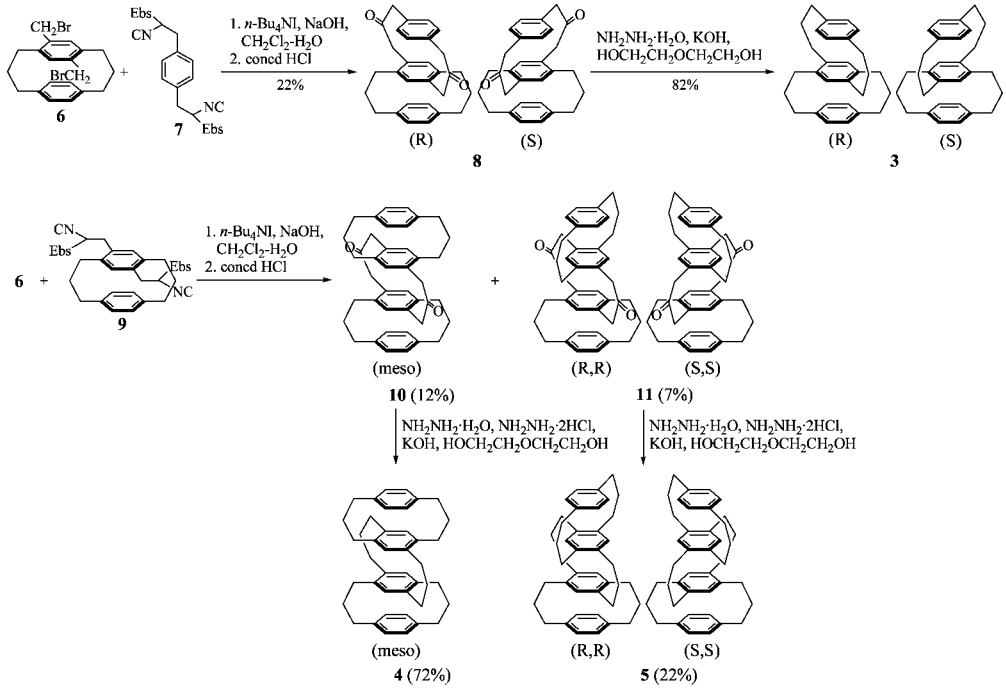

(racemic) were obtained in 12% and 7% yield, respectively. The isolated yield of **11** was low because of its good solubility in organic solvents. The modified Wolff−Kishner reduction of each of the diones afforded four-layered [3.3]PCPs **4** (meso, 72%) and **5** (racemic, 22%), respectively. Resolution of **5** (racemic) by HPLC separation with a chiral stationary phase is in progress, and their absolute configurations and chiroptical properties will be reported elsewhere.

^{1}H NMR Spectral Properties. Figure 2 shows the selected ^{1}H NMR data for multilayered [3.3]PCPs and the corresponding multilayered [2.2]PCPs as references.[18] The outer aromatic protons (H_a and $H_{a'}$) of multilayered [3.3]PCPs exhibit slight upfield shifts as the number of layers increases due to the ring current effect of the facing benzene rings, but the magnitude is smaller than that of the corresponding multilayered [2.2]PCPs. The H_i protons also show similar phenomena. All H_a and $H_{a'}$ protons of three- and four-layered [3.3]PCPs appear as double-doublets (J_{ortho} and J_{meta}) due to the influence of the benzylic protons of the trimethylene bridges at the pseudogeminal position. The H_a proton undergoes the steric compression effect of the benzylic protons at the pseudogeminal position and appears at slightly lower field than the corresponding $H_{a'}$ protons. Similarly, the H_i protons of racemic **5** are slightly deshielded ($\Delta\delta$ 0.05 ppm) compared to the corresponding protons of meso **4** due to this effect. On the other hand, the steric compression effect was not observed in the outer aromatic protons (H_a) of the multilayered [2.2]PCPs because the distance between the H_a proton and the benzylic protons of the bridge at the pseudogeminal position lengthens due to the bending of the inner benzene ring into a boat shape. In the multilayered [3.3]PCP-diones, the aromatic protons of **8** and the H_i protons of **10** and **11** are slightly deshielded compared to the corresponding protons of the multilayered [3.3]PCPs. A similar steric compression effect was observed in the H_i protons of **11** compared to the corresponding protons of **10**.

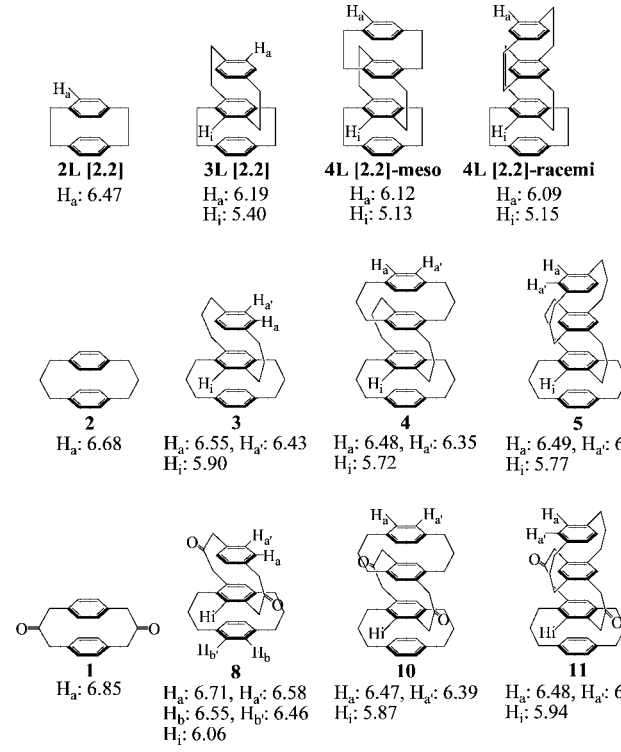

FIGURE 2. Selected ^{1}H NMR data of multilayered [3.3]PCPs and multilayered [2.2]PCPs[18] in $CDCl_3$.

X-ray Structural Analysis. To examine the structural properties of the multilayered [3.3]PCPs, we carried out their single-crystal X-ray structural analyses. The crystal data are summarized in Table S1 (Supporting Information). Figure 3 shows the molecular structure of three-layered [3.3]PCP-dione **8** (−160 °C). The ORTEP drawing shows that the [3.3]PCP unit assumes a chair conformation, whereas the [3.3]PCP-dione unit assumes a boat one (Figure 3A). The three benzene rings are stacked with the distances of 3.33 Å for the [3.3]PCP-dione unit and

(18) Otsubo, T.; Mizogami, S.; Sakata, Y.; Misumi, S. *Bull. Chem. Soc. Jpn.* **1973**, *46*, 3831–3835.

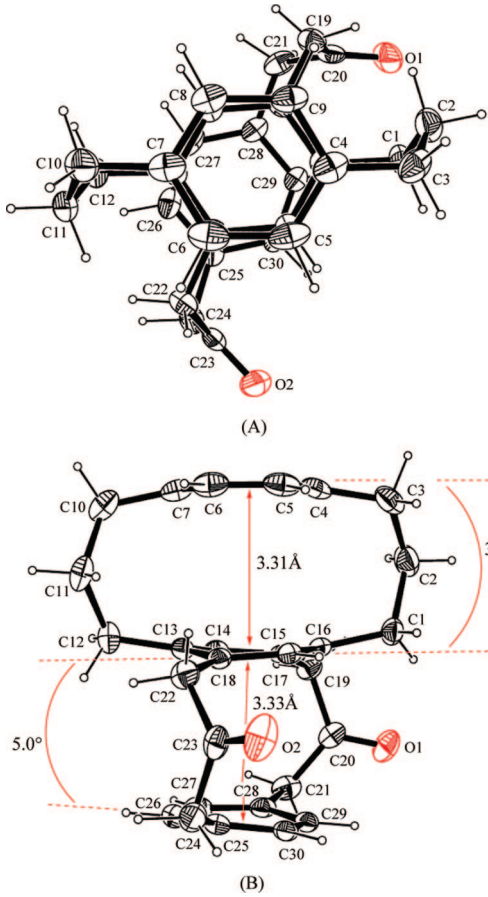

FIGURE 3. ORTEP drawing of the molecular structures of three-layered [3.3]PCP-dione **8** (−160 °C): top (A) and side (B) views.

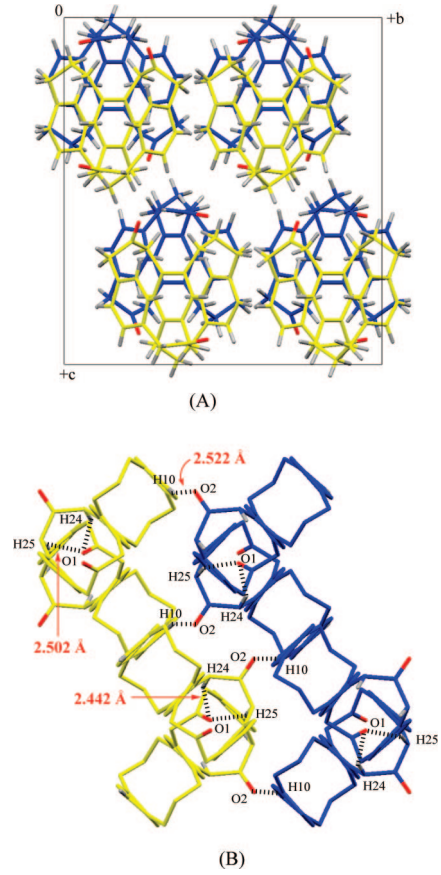

FIGURE 4. The short contacts of three-layered [3.3]PCP-dione **8**. (A) The crystal-packing diagram along the *a*-axis. The carbon atoms are represented as blue (far side) and yellow (this side). (B) Hydrogen bonds between carbonyl oxygen (O1) and benzylic protons (H24 and H25) and carbonyl oxygen (O2) and aromatic proton (H10) along the *c*-axis. Hydrogen atoms H10, H24, and H25 only are represented for clarity.

3.31 Å for the [3.3]PCP unit, and these values are comparable to those of **1** (3.33 Å)[19] and **2** (3.31 Å),[20] respectively. The benzene rings of the [3.3]PCP unit overlap each other, but the third benzene ring of the dione unit slightly deviates from complete stacking. The tilt of the benzene rings is 3.4° for the [3.3]PCP unit, whereas it is 5.0° for the [3.3]PCP-dione unit.

In the crystal-packing diagram of **8** (Figure 4A), two molecules are overlapped along the *a*-axis. Three kinds of hydrogen bonds are observed along the *c*-axis [O1−H24 (2.442 Å), O1−H25 (2.502 Å), and O2−H10 (2.522 Å)] (Figure 4B), and the distances of all the hydrogen bonds are shorter than the sum of the van der Waals radii[21] of a hydrogen atom (1.20 Å) and an oxygen atom (1.40 Å).

The crystal structure of the (*R*)-isomer of three-layered [3.3]-PCP **3** has already been reported,[3] and we report here the molecular structure of the racemate of **3** (Figure 5, −160 °C). In the unit cell, a pair of (*R*)- and (*S*)-isomers is present and only the (*R*)-isomer is shown in the ORTEP drawing, where both [3.3]PCP units assume the boat conformation different from the parent **2** (chair). The boat/boat conformation of **3** was predicted to be the most stable among the possible seven stable isomers concerned with the trimethylene bridge based on DFT calculations using the B3LYP functional and 6-31G* basis set.[3] The three benzene rings are completely stacked, and the transannular distances of two [3.3]PCP units are 3.27 and 3.28 Å, which are shorter than the corresponding two-layered [3.3]-PCP **2** (3.31 Å). In the crystal-packing diagram of **3** (Figure 6), the CH/π interactions of the benzene rings with the trimethylene protons between (*R*)- and (*S*)-isomers are observed, and their average value is 2.86 Å, which is approximately the sum of the van der Waals radii.[21] Thus each isomer is arranged regularly and stacked alternately.

Figure 7 shows the molecular structure of four-layered [3.3]-PCP-dione **10** (meso, −160 °C). The ORTEP drawing shows that the two [3.3]PCP units assume boat conformations different from that of the parent **2**, whereas the [3.3]PCP-dione unit has a chair conformation comparable to that of the parent **1** (Figure 7A). The benzene rings of the central [3.3]PCP-dione unit are parallel, while the outer benzene rings deviate from complete stacking with a tilting of 6.1° (Figure 7B). The transannular distances are 3.28 Å for the [3.3]PCP unit and 3.25 Å for the dione unit, and these values are shorter than the corresponding distances of **8** and the parents **1** and **2**. In the crystal-packing diagram of **10** (Figure 8), a molecule interacts with four neighboring molecules by intermolecular hydrogen bonds (2.494 Å) between the carbonyl oxygen atom (O1) and the benzylic proton (H12).

Figure 9 shows the molecular structure of four-layered [3.3]-PCP **4** (meso, −150 °C), where the trimethylene bridges are highly flexible and disordered even at −150 °C. The four benzene rings are almost overlapped, but the two outer benzene

(19) X-ray structural analysis of **1** is shown in the Supporting Information.
(20) Gantzel, P. K.; Trueblood, K. N. *Acta Crystallogr.* **1965**, *18*, 958–968.
(21) PaulingL. *The Nature of the Chemical Bonds* ; Cornell University Press: Ithaca, New York, 1960; p 260.

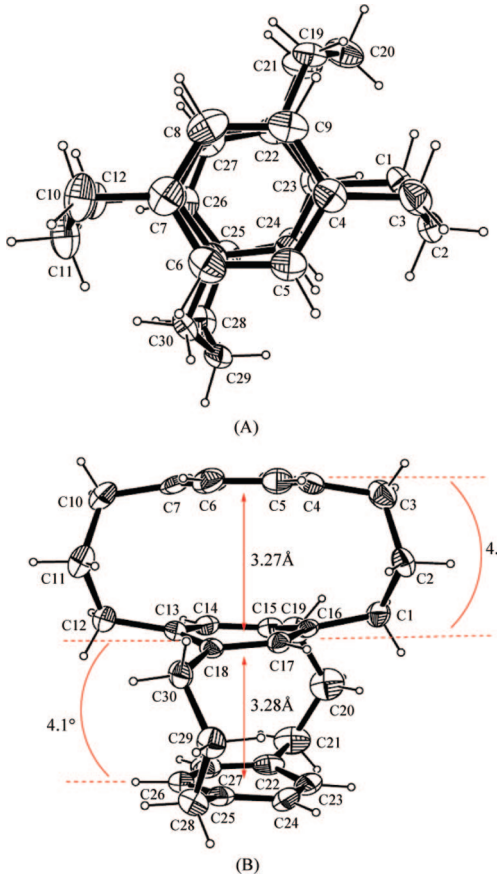

FIGURE 5. ORTEP drawing of the molecular structures of three-layered [3.3]PCP **3** represented by the (*R*)-isomer (−160 °C): top (A) and side (B) views.

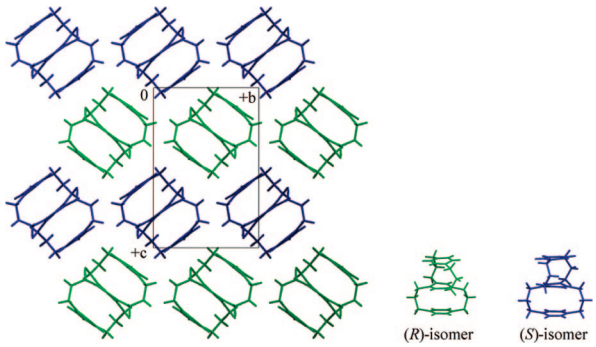

FIGURE 6. Molecular stacking form of three-layered [3.3]PCP **3** (racemate) view along the *a*-axis.

rings are tilted by 2.5° toward the inner benzene ring. The transannular distances are 3.31 Å for the outer [3.3]PCP units and 3.29 Å for the inner one. In the crystal-packing diagram of **4** (Figure 10), a molecule interacts with four stacked molecules via CH/π interactions between the benzene carbons and benzylic protons. With regard to the distortion of the benzene rings (Figure 11), the outer benzene rings are deformed into a boat form while the inner benzene rings assume a twist form in multilayered [3.3]PCPs. The torsion angles of the mean value are listed in Table 1 along with those of multilayered [2.2]PCPs as references. The torsion angles of multilayered [3.3]PCPs (5.2−7.0° for *a*, 3.5−5.4° for *b*, and 6.4−8.1° for *c*) are approximately half compared with those of the corresponding

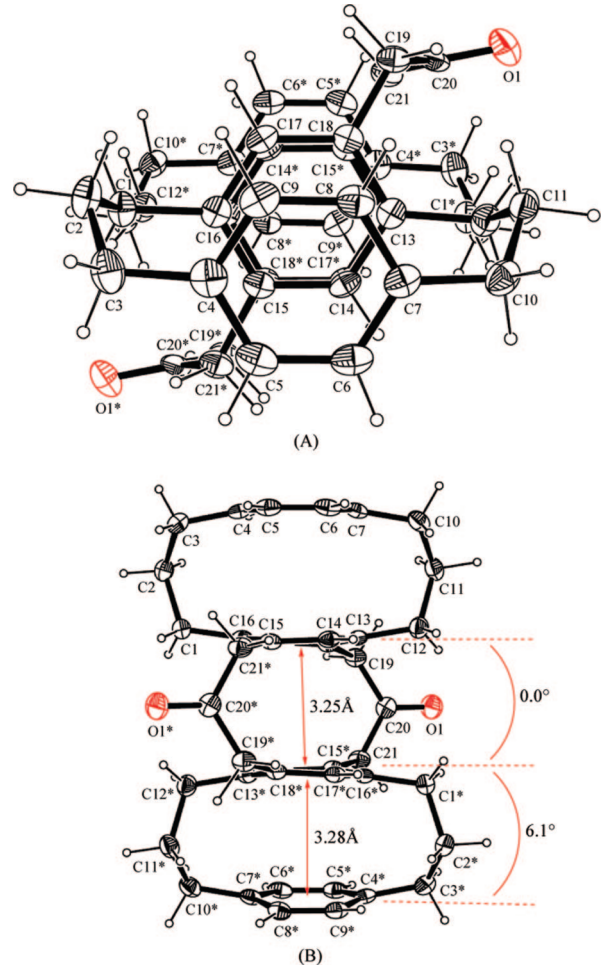

FIGURE 7. ORTEP drawing of the molecular structures of four-layered [3.3]PCP-dione **10** (−160 °C): top (A) and side (B) views.

[2.2] analogues, indicating less deformation of the benzene rings of the [3.3]PCP.

Electronic Spectra. Figure 12 denotes the electronic absorption spectra of the multilayered [3.3]PCPs **2**−**5** in THF. Bathochromic shift and hyperchromic effect are observed as the layers are increased, but the magnitude is more significant for two to three than for three to four. The absorption curves become similar in shape and almost a straight line as the number of layers increases. Racemic **5** shows a slightly more significant bathochromic shift and hyperchromic effect compared to those of meso **4**, and this may be attributable to more effective electronic interaction in the helical arrangement of the trimethylene bridges of **5**. In the electronic spectra of multilayered [3.3]PCP-diones, a similar but more significant bathochromic shift and hyperchromic effect are observed as the number of layers increases (Figure 13), and characteristic n−π* bands are observed in the region of 280−300 nm.[25] The electronic spectra did not show any concentration dependence in the range of 1.0 × 10^{-4}−10 × 10^{-4} M for **4** and 8.4 × 10^{-5}−42 × 10^{-5} M for **10** in THF, respectively (Figure S33, Supporting Information).

(22) (a) Brown, C. J. *J. Chem. Soc.* **1953**, 3265–3270. (b) Hope, H.; Bernstein, J.; Trueblood, K. N. *Acta Crystallogr., Sect. B* **1972**, *28*, 1733–1743.
(23) Otsubo, T.; Horita, H.; Koizumi, Y.; Misumi, S. *Bull. Chem. Soc. Jpn.* **1980**, *53*, 1677–1682.
(24) Mizuno, H.; Nishiguchi, K.; Otsubo, T.; Misumi, S.; Morimoto, N. *Tetrahedron Lett.* **1972**, *13*, 4981–4984.
(25) (a) Cram, D. J.; Helgeson, R. C. *J. Am. Chem. Soc.* **1966**, *88*, 3515–3521. (b) Cookson, R. C.; Wariyar, N. S. *J. Chem. Soc.* **1956**, 2302–2311.

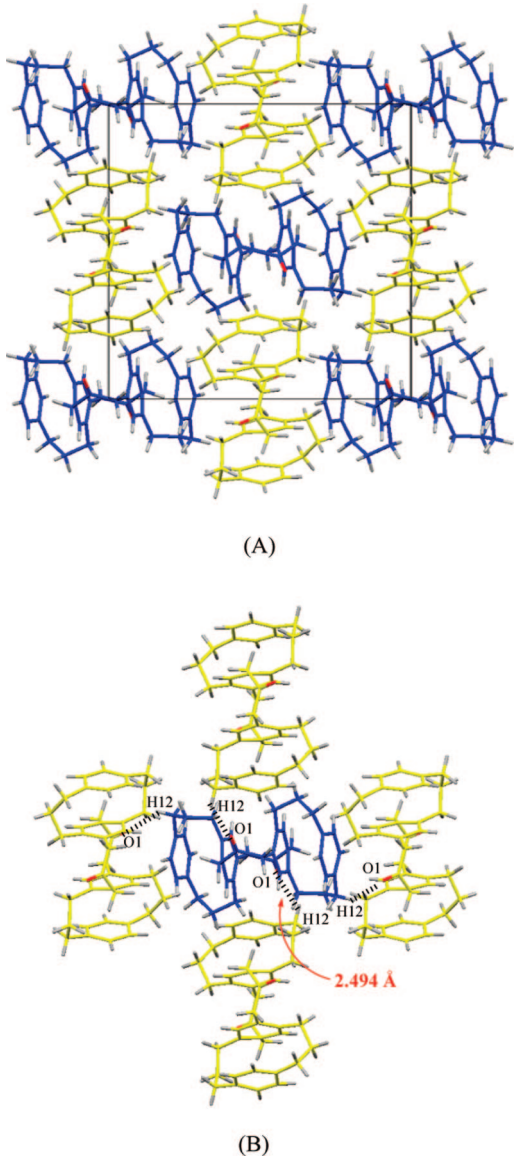

FIGURE 8. The short contacts of four-layered [3.3]PCP-dione **10** viewed along the *c*-axis. (A) The crystal-packing diagram. (B) Hydrogen bonds between the carbonyl oxygen (O1) and the benzylic proton (H12).

Charge Transfer Interaction. The π-electron donating ability of the cyclophanes can be qualitatively estimated by measurement of the λ_{max} of the CT band between a cyclophane and TCNE. In the two-layered [3.3]CPs, [3.3]PCP **2** (λ_{max} 606 nm) shows a significantly stronger CT interaction than [3.3]MCP (λ_{max} 509 nm) and [3.3]MPCP (λ_{max} 510 nm). The multilayered [3.3]MCPs [λ_{max} 550 (three layers)−588 (six layers) nm in $CHCl_3$] showed moderate electron-donating ability[2] compared to multibridged [3_n]CPs [λ_{max} 594 {[3_3](1,3,5)CP}−728 {[3_6](1,2,3,4,5,6)CP} nm in $CHCl_3$].[15b] The CT absorption spectra of the multilayered [3.3]PCPs **2**−**5** and multilayered [3.3]PCP-diones **1**, **8**, **10**, and **11** are shown in Figure 14 and Supporting Information Figure S26, respectively, and the λ_{max} values of the CT bands are summarized in Table 2. The 1:1 stoichiometry of the CT complex was confirmed (Figures S27 and S28, Supporting Information). The λ_{max} shows a significant red shift with an increasing number of layers [**2**: λ_{max} 606 nm; **3**: 670 nm; **4** (meso): 716 nm; and **5** (racemic): 723 nm in $CHCl_3$], but the changes in the λ_{max} from two to three (64 nm) and three to four (46 and 53 nm) become smaller. The magnitude of the

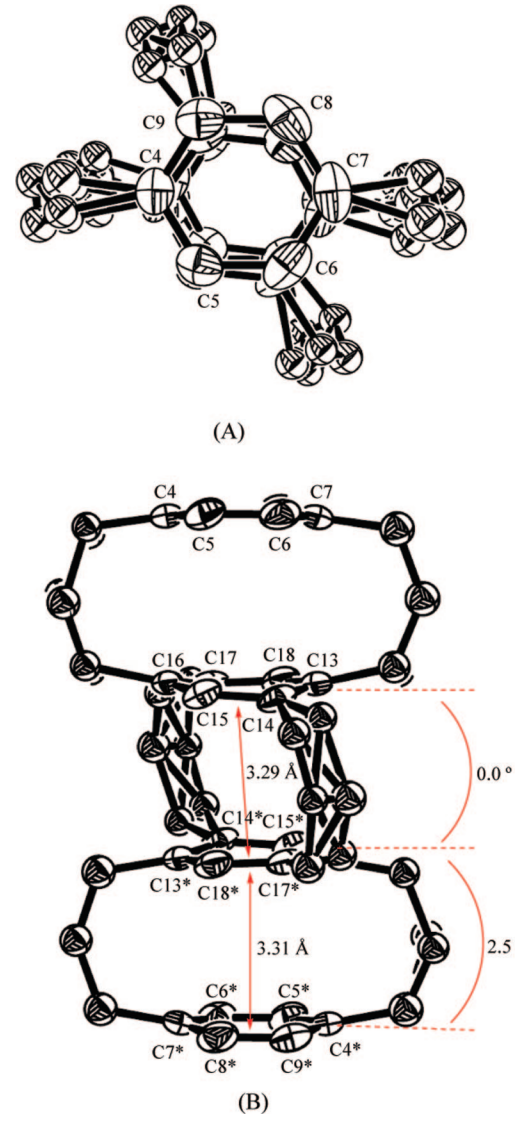

FIGURE 9. ORTEP drawing of the molecular structures of four-layered [3.3]PCP **4** (−150 °C): top (A) and side (B) views. Hydrogen atoms are omitted for clarity.

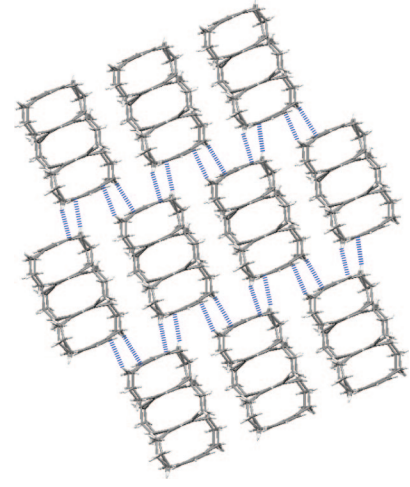

FIGURE 10. CH/π Interaction of four-layered [3.3]PCP **4**.

electron-donating ability of multilayered [3.3]PCPs is more significant than that of multilayered [3.3]MCPs. In the UV/vis spectra,

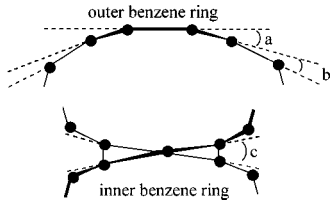

FIGURE 11. Distortion of benzene rings in multilayered [*m.m*]PCPs.

TABLE 1. Torsion Angles of Multilayered [*m.m*]PCPs.

multilayered [3.3]PCPs	*a* (deg)	*b* (deg)	*c* (deg)
two-layered [2.2]PCP[22]	13	11	
monobromo three-layered [2.2]PCP[23]	12.2	11.2	13.6
tetramethyl four-layered [2.2]PCP[24]	12.7	11.2	13.4
two-layered [3.3]PCP **2**[20]	6.4	3.6	
three-layered [3.3]PCP **3**	5.2	4.2	8.1
four-layered [3.3]PCP **4**	6.3	5.4	6.8
two-layered [3.3]PCP-dione **1**[19]	6.1	4.0	
three-layered [3.3]PCP-dione **8**	6.8,[a] 5.6[b]	3.7,[a] 5.4[b]	7.5
four-layered [3.3]PCP-dione **10**	7.0	3.5	6.4

[a] Tortion angles of the [3.3]PCP unit. [b] Tortion angles of [3.3]PCP-dione unit.

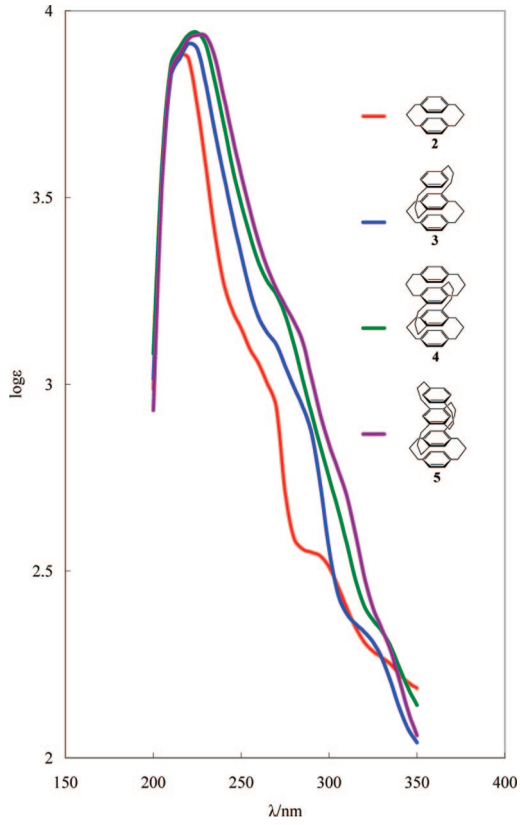

FIGURE 12. Electronic spectra of multilayered [3.3]PCPs **2**−**5** in THF.

we noted that **5** (racemic) shows a slightly more significant bathochromic shift and hyperchromic effect than **4** (meso), suggesting more effective electronic interaction in **5** than in **4**. The slight red shift of the CT absorption band (λ_{max} 723 nm) of **5** compared to that of **4** (λ_{max} 716 nm) also suggests that the helical arrangement of the trimethylene bridges is more effective in the CT interaction.

In the multilayered [3.3]PCP-diones, the λ_{max} appears at 594−629 nm for three- to four-layered [3.3]PCP-diones **8**, **10**, and **11**, and these values are comparable to those of two-layered

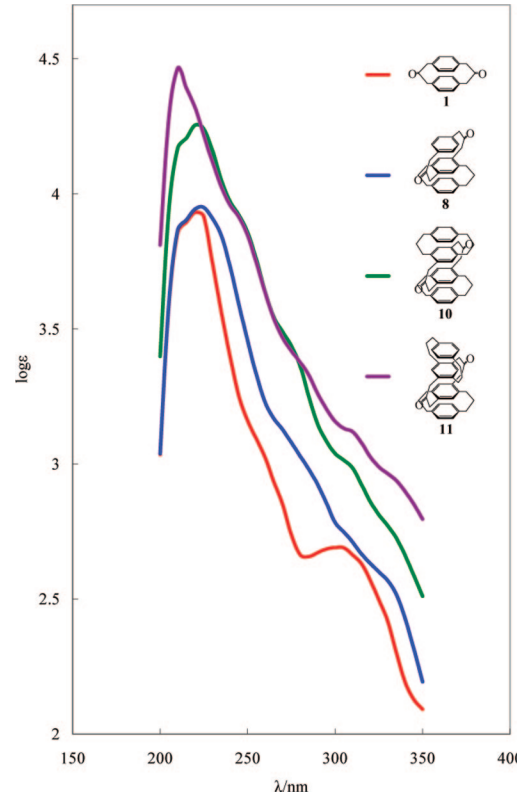

FIGURE 13. Electronic spectra of multilayered [3.3]PCP-diones **1**, **8**, **10**, and **11** in THF.

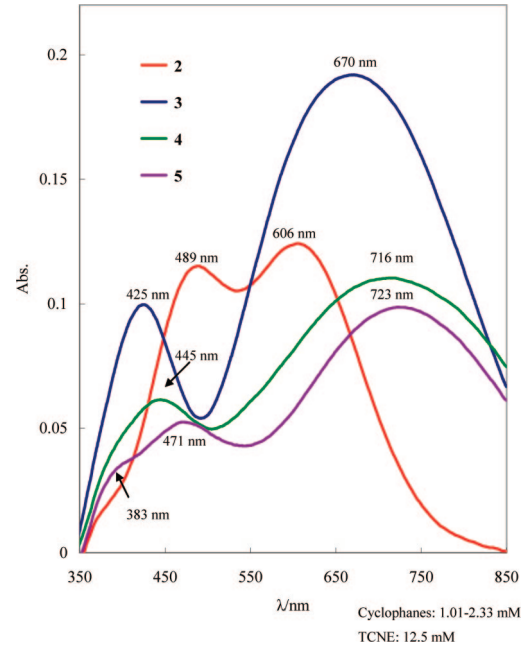

FIGURE 14. Charge-transfer absorption bands of multilayered [3.3]PCPs **2**−**5** in $CHCl_3$.

[3.3]PCP **2** (606 nm). This result suggests that the $-CH_2COCH_2-$ bridge serves as an insulator irrespective of transannular distances similar to those of the [3.3]PCP unit and [3.3]PCP-dione unit. This indicates that the $-CH_2COCH_2-$ bridge interferes with the electronic interaction between the completely overlapped benzene rings. A similar result that the [3.3]MCP-dione moiety having an antigeometry in multilayered [3.3]MCPs interferes with transannular π-electronic interaction suggests the

TABLE 2. CT Bands of Multilayered [3.3]PCPs-TCNE in $CHCl_3$.

multilayered [3.3]PCPs	TCNE complex λ_{max} (nm)
two-layered [3.3]PCP **2**[a]	606, 489
three-layered [3.3]PCP **3**[b]	670, 425
four-layered [3.3]PCP **4**	716, 445
four-layered [3.3]PCP **5**	723, 471, 383[c]
two-layered [3.3]PCP-dione **1**	
three-layered [3.3]PCP-dione **8**	594, 392
four-layered [3.3]PCP-dione **10**	613, 427
four-layered [3.3]PCP-dione **11**	629, 435

[a] The longest wavelength in CH_2Cl_2 was 599 nm, in ref 11a. [b] 655 and 421 nm in CH_2Cl_2, in ref 12b. [c] Shoulder

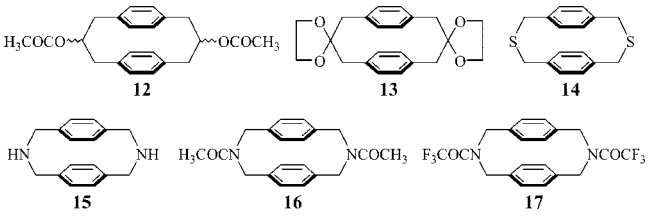

FIGURE 15. Two-Layered [3.3]PCPs **12**−**17**.

importance of the through-bond interaction.[2] These results suggest that the electronic interaction in multilayered [3.3]MCPs and [3.3]PCPs should be significantly affected by "through-bond" interaction rather than "through-space" interaction. An analysis of this problem by means of the Natural Bond Orbital (NBO) method[26] will be reported elsewhere.

To test the dependence of the electron-donating ability (λ_{max} of the CT band) on the kind of central atoms of the $-CH_2XCH_2-$ bridge in [3.3]PCPs, the λ_{max} of the CT band with TCNE was measured and the HOMO energy was estimated by the DFT (B3LYP/6-31G* level[27]) calculations (Gaussian 03[28]). The magnitude of the CT interaction is strongly affected by the central atoms of the $-CH_2XCH_2-$ bridges (X = C, N, S) and the substituents on the atoms (Figure 15 and Supporting Information Figure S29). The $-CH_2CH_2CH_2-$ bridge (**2**) is the most effective for CT interaction in the [3.3]PCPs, but the introduction of an acetoxy group to the central sp^3 carbon of the $-CH_2CH_2CH_2-$ bridge (**12**) slightly lowers the electron-donating ability of **2**, and introduction of acetal groups (**13**) further lowers the donating ability, while [3.3]PCP-dione **1** does not show any CT band. The nitrogen-containing [3.3]PCPs (**15**−**17**) do not show clear CT bands. In principle, this tendency corresponds with the HOMO energy level of the [3.3]PCPs (Table 3 and Supporting Information Figures S30 and S31), but the acetal **13** (−5.36 eV) shows much lower electron-donating ability irrespective of the higher HOMO level of **2**. In 2,11-dithia[3.3]PCP **14**, the HOMO level is greatly lowered (−5.90 eV). 2,11-Diaza[3.3]PCP **15** shows an HOMO level (−5.52 eV) comparable to that of the parent **2**, but we could not measure the λ_{max} because of the insolubility of the complex with TCNE, whereas the HOMO level is significantly lowered by the introduction of acetyl (**16**: −6.04 eV) and trifluoroacetyl groups (**17**: −6.36 eV) to the nitrogen atoms of **15**. Thus we confirmed that the electron-donating ability of [3.3]PCPs is strongly dependent on the central atom of the $-CH_2XCH_2-$ bridge and the substituents on the central atom.

Electrochemical Properties. To find a correlation between the λ_{max} of the CT bands with TCNE and the oxidation potentials of multilayered [3.3]PCPs, the CV in $Cl_2CHCHCl_2$ was measured (Figure 16 and Supporting Information Figure S32). The oxidation potentials and the λ_{max} of the CT bands of multilayered [3.3]PCPs are summarized in Table 4 along with the data for multibridged [3_n]CPs as references.[15b,29] Three- and four-layered [3.3]PCPs **3** (racemic), **4** (meso), and **5** (racemic) show reversible redox processes, whereas two-layered [3.3]PCP **2** and diones **1**, **8**, **10**, and **11** show irreversible CV profiles. The first half-wave oxidation potentials [$E_{1/2}(I)$] are +0.61 V for **3**, +0.40 V for **4**, and +0.44 V for **5** (vs Fc/Fc^+), respectively, and the data are comparable to the λ_{max} values of the TCNE complexes of **3**, **4**, and **5**. The $E_{1/2}(I)$ of four-layered [3.3]PCPs **4** and **5** are almost comparable to, but slightly less than, that of [3_6]CP ($E_{1/2}$ +0.39 V vs Fc/Fc^+, $Cl_2CHCHCl_2$).[29] Table 4 shows very good correlation of the oxidation potentials of the cyclophanes and the λ_{max} of the CT bands of the cyclophane−TCNE complexes, and this indicates that the magnitude of the CT interactions is mostly determined by the electron-donating ability (oxidation potential) of a cyclophane, and similar donor−accepter interactions are operative in multilayered and multibridged cyclophanes. Thus, direct comparison of the π-electron-donating ability of multilayered and multibridged [3.3]cyclophanes is now becoming feasible.

3. Conclusions

We have successfully synthesized up to four-layered [3.3]PCPs using the EbsMIC method, and a similar repetition of a series of reactions may lead to the formation of higher five- and six-layered [3.3]PCPs. For the synthesis of the optically active five- and six-layered [3.3]PCPs, synthesis of the coupling precursors, bis(bromomethyl)-(*R*)-two-layered, and bis(bromomethyl)-(*R*,*R*)-three-layered [3.3]PCPs is required, and the synthesis of these chiral bis(bromomethyl)[3.3]PCPs is in progress. In the ^1H NMR spectra, all the aromatic protons showed an upfield shift caused by the stacked benzene rings that could affect not only the neighboring rings but also more remote ones, but the magnitude of the upfield shift was smaller than that of the [2.2]homologues. In addition, the four-layered [3.3]PCPs **4** (meso) and **5** (recemic) exhibited isomeric properties inherent to their helical structures. The X-ray structural analysis revealed that the [3.3]PCP unit assumes a chair conformation comparable to that of the parent [3.3]PCP **2**, while the three-layered [3.3]PCP **3** assumes a boat/boat conformation. In the four-layered [3.3]PCP-dione **10**, both the outer [3.3]PCP units have a boat conformation, whereas the inner unit has a chair conformation. From these results, [3.3]PCP and the dione units are flexible and can change their conformation so as to adopt a crystal packing force. In the four-layered

(26) Carpenter, J. E.; Weinhold, F. *J. Mol. Struct.* **1988**, *169*, 41–62.
(27) (a) Becke, A. D. *J. Chem. Phys.* **1993**, *98*, 5648–5652. (b) Lee, C.; Yang, W.; Parr, R. G. *Phys. Rev. B* **1988**, *37*, 785–789.
(28) Frisch, M. J.; Trucks, G. W.; Schlegel, H. B.; Scuseria, G. E.; Robb, M. A.; Cheeseman, J. R.; Montgomery, J. A., Jr.; Vreven, T.; Kudin, K. N.; Burant, J. C.; Millam, J. M.; Iyengar, S. S.; Tomasi, J.; Barone, V.; Mennucci, B.; Cossi, M.; Scalmani, G.; Rega, N.; Petersson, G. A.; Nakatsuji, H.; Hada, M.; Ehara, M.; Toyota, K.; Fukuda, R.; Hasegawa, J.; Ishida, M.; Nakajima, T.; Honda, Y.; Kitao, O.; Nakai, H.; Klene, M.; Li, X.; Knox, J. E.; Hratchian, H. P.; Cross, J. B.; Bakken, V.; Adamo, C.; Jaramillo, J.; Gomperts, R.; Stratmann, R. E.; Yazyev, O.; Austin, A. J.; Cammi, R.; Pomelli, C.; Ochterski, J. W.; Ayala, P. Y.; Morokuma, K.; Voth, G. A.; Salvador, P.; Dannenberg, J. J.; Zakrzewski, V. G.; Dapprich, S.; Daniels, A. D.; Strain, M. C.; Farkas, O.; Malick, D. K.; Rabuck, A. D.; Raghavachari, K.; Foresman, J. B.; Ortiz, J. V.; Cui, Q.; Baboul, A. G.; Clifford, S.; Cioslowski, J.; Stefanov, B. B.; Liu, G.; Liashenko, A.; Piskorz, P.; Komaromi, I.; Martin, R. L.; Fox, D. J.; Keith, T.; Al-Laham, M. A.; Peng, C. Y.; Nanayakkara, A.; Challacombe, M.; Gill, P. M. W.; Johnson, B.; Chen, W.; Wong, M. W.; Gonzalez, C.; Pople, J. A. *Gaussian 03*, Revision C.02; Gaussian, Inc.: Wallingford, CT, 2004.
(29) Yasutake, M.; Koga, T.; Sakamoto, Y.; Komatsu, S.; Zhou, M.; Sako, K.; Tatemitsu, H.; Onaka, S.; Aso, Y.; Inoue, S.; Shinmyozu, T. *J. Am. Chem. Soc.* **2002**, *124*, 10136–10145.

TABLE 3. Predicted Energy of the HOMO (eV) in Multilayered [3.3]PCPs (DFT, B3LYP/6-31G* level)

1	2	12	13	14	15	16	17	3	4	5	8	10	11
−5.83	−5.48	−5.71	−5.36	−5.90	−5.52	−6.04	−6.36	−5.14	−4.96	−4.99	−5.44	−5.28	−5.30

[3.3]PCP **4**, the trimethylene bridges are highly flexible and disordered at −150 °C. The benzene rings of the [3.3]PCPs are far less distorted compared to those of the [2.2]system. In the electronic spectra, bathochromic and hyperchromic shifts were observed, but the magnitude was smaller and showed structureless absorption curves as the number of layers increased. In the CT interaction of multilayered [3.3]PCPs, the λ_{max} shifted to a longer wavelength with the increase in the number of layers. In contrast, all multilayered [3.3]PCP-diones **8**, **10**, and **11** showed interactions similar to those of two-layered[3.3]PCP **2**. These results suggested the importance of the through-bond π-electronic interaction, and we confirmed that the electron-donating ability of [3.3]PCPs is strongly dependent on the central atom of the $-CH_2XCH_2-$ bridge and the substituent on the central atoms. In the electrochemical properties, three- and four-layered [3.3]PCPs **3** (racemic), **4** (meso), and **5** (racemic) showed reversible redox processes, and **4** and **5** showed comparable electron-donating ability [$E_{1/2}(I)$; +0.40 (**4**) and +0.44 (**5**) V (vs Fc/Fc$^+$)] to that of [3$_6$]CP. Very good correlation between the λ_{max} of the CT bands with TCNE and the $E_{1/2}$ values is observed, and the electron-donating ability of the multilayered [3.3]PCPs can now be compared to those of multibridged [3$_n$]CPs.

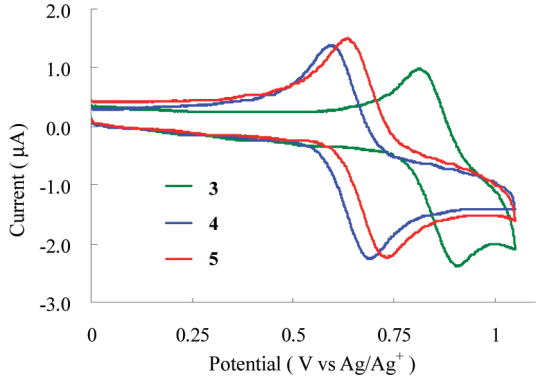

FIGURE 16. Cyclic voltammograms of multilayered [3.3]PCPs **3**, **4**, and **5** in $Cl_2CHCHCl_2$/0.1 M Bu_4NPF_6 observed at a potential scan rate of 20 mV s^{-1}

TABLE 4. Oxidation Potentials in $Cl_2CHCHCl_2$[a] and the λ_{max} Values of the CT Bands in $CHCl_3$

CPs	$E_{1/2}(I)$ (V vs Fc/Fc$^+$)	$E_{pa}(I)$ (V vs Ag/AgCl)	$E_{pa}(I)$ (V vs Fc/Fc$^+$)	TCNE complex λ_{max} (nm)
[3.3]PCP **2**		+1.13 (sh)	+0.88	606
three-layered [3.3]PCP **3**	+0.61	+0.91	+0.66	670
four-layered [3.3]PCP **4**	+0.40	+0.69	+0.44	716
four-layered [3.3]PCP **5**	+0.44	+0.73	+0.48	723
two-layered dione **1**		+1.13	+0.87	
three-layered dione **8**		+1.14 (sh)	+0.89	594
four-layered dione **10**		+1.06	+0.81	613
four-layered dione **11**		+1.12	+0.86	629
[3$_3$](1,3,5)CP		+1.31	+1.01	594
[3$_4$](1,2,3,5)CP	+0.69	+1.04	+0.74	632
[3$_4$](1,2,4,5)CP	+0.66	+1.02	+0.72	
[3$_5$]CP	+0.51	+0.87	+0.57	684
[3$_6$]CP	+0.39	+0.73	+0.43	728

[a] Containing 0.1 M Bu_4NPF_6, scan rate 20 mV/s. sh: shoulder.

We will continue the optical resolution and determination of the absolute configuration of four-layered [3.3]PCP **5** (racemic) by comparison of the observed CD spectra with the calculated ones. Detailed analysis of through-space and through-bond interaction in the three- to four-layered [3.3]PCPs will also be reported by one of our collaborators.

4. Experimental Section

5,8-Bis(bromomethyl)[3.3]paracyclophane **6** and EbsMIC adduct **7** were synthesized by similar procedures as described in ref 3.

5,8-Bis[2-isocyano-2-(ethylbenzenesulfonyl)ethyl][3.3]paracyclophane, 9. A mixture of *n*-Bu_4NI (810 mg) and NaOH (18 g) dissolved in 42 mL of water and CH_2Cl_2 (67 mL) was cooled in an ice bath with stirring. To the mixture was added in one portion of a CH_2Cl_2 (45 mL) solution of EbsMIC **7** (7.36 g, 35.2 mmol). After 30 min, the bromide **6** (4.49 g, 10.6 mmol) dissolved in CH_2Cl_2 (67 mL) was added in one portion. The mixture was stirred for 1 h in the ice bath, then at room temperature for 3 h. The reaction mixture was washed with water, dried with $MgSO_4$, and concentrated to a volume of ca. 50 mL at room temperature. The concentrate was diluted with MeOH (100 mL) and stored in a freezer. The precipitate was collected by filtration and washed with MeOH. Purification of the crude product by silica gel column chromatography with CH_2Cl_2 (R_f 0.57) afforded two-layered EbsMIC adduct **9** (5.75 g, 80%). **9**: white powder (CH_2Cl_2/MeOH), mp 137 °C (dec); IR (KBr) ν 2134 (NC), 1334 and 1153 (SO_2) cm^{-1}; ^{1}H NMR (300 MHz, $CDCl_3$) δ 1.28 (t, J = 7.6 Hz, 6H, CH_2CH_3), 1.9−2.2 (m, 4H, $CH_2CH_2CH_2$), 2.5−2.7 (m, 6H, $CH_2CH_2CH_2$ and CH_2CH), 2.77 (q, J = 7.6 Hz, 4H, CH_2CH_3), 2.8−2.9 (m, 4H, $CH_2CH_2CH_2$), 3.81 (dd, J = 13.9, 2.1 Hz, 2H, CH_2CH), 4.30 (dd, J = 11.5, 2.2 Hz, 2H, CH_2CH), 6.59 (s, 2H, ArH), 6.68 (dd, J = 7.8, 1.6 Hz, 2H, ArH), 6.77 (dd, J = 7.8, 1.6 Hz, 2H, ArH), 7.46 (d, J = 8.5 Hz, 4H, ArH), 7.93 (d, J = 8.4 Hz, 4H, ArH); HRMS (FAB) *m*/*z* calcd for $C_{40}H_{42}N_2O_4S_2$ 678.2586 [M$^+$], found 678.2590. Anal. Calcd for $C_{40}H_{42}N_2O_4S_2$: C, 70.77; H, 6.24; N, 4.13. Found: C, 70.53; H, 6.18; N, 4.06.

Four-Layered [3.3]Paracyclophane-Diones C_{2h} Isomer 10 and D_2 Isomer 11. To a refluxing mixture of *n*-Bu_4NI (1.0 g) and NaOH (21 g) dissolved in 50 mL of water and CH_2Cl_2 (700 mL) was added dropwise a mixture of the EbsMIC adduct **9** (2.02 g, 2.37 mmol) and the bromide **6** (1.26 g, 2.37 mmol) dissolved in CH_2Cl_2 (500 mL) over a period of 8 h, and the mixture was refluxed for an additional 12 h. After cooling, the reaction mixture was washed with water then concentrated to a volume of ca. 300 mL, and the concentrate was treated with concentrated HCl (30 mL) for 2 h at room temperature. The mixture was washed with brine, dried with $MgSO_4$, and concentrated to dryness to give the crude mixture of isomeric ketones, meso **10** and racemic **11**. The less soluble **10** was separated from the readily soluble **11** by treatment with acetonitrile.

Purification of the crude **10** by silica gel column chromatography with benzene (R_f 0.17) afforded the C_{2h} isomer **10** (239 mg, 12%). **10**: colorless plates (benzene), mp 247 °C dec; IR (KBr) ν 1686 (C=O) cm^{-1}; ^{1}H NMR (300 MHz, $CDCl_3$) δ 1.7−1.9 (m, 8H, $CH_2CH_2CH_2$), 2.2−2.4 (m, 4H, $CH_2CH_2CH_2$), 2.49 (t, J = 5.3 Hz, 8H, $CH_2CH_2CH_2$), 2.65−2.85 (m, 4H, $CH_2CH_2CH_2$), 3.26 (d, J =

13.0 Hz, 4H, CH_2COCH_2), 3.69 (d, J = 13.0 Hz, 4H, CH_2COCH_2), 5.87 (s, 4H, ArH), 6.39 (dd, J = 7.7, 1.5 Hz, 4H, ArH), 6.47 (dd, J = 7.7, 1.5 Hz, 4H, ArH); ^{13}C NMR (75 MHz) δ 28.3, 32.6, 35.4, 49.3, 127.2, 129.6, 131.4, 133.6, 136.3, 138.0, 207.7; HRMS (FAB) m/z calcd for $C_{42}H_{44}O_2$ 580.3341 [M^+], found 580.3337. Anal. Calcd for $C_{42}H_{44}O_2$: C, 86.85; H, 7.64. Found: C, 86.49; H, 7.63.

Purification of the crude **11** by silica gel column chromatography with benzene (R_f 0.17) afforded the pure D_2 isomer **11** (105 mg, 7%). **11**: colorless needles (EtOH), mp 248 °C dec; IR (KBr) ν 1695 (C=O) cm^{-1}; ^{1}H NMR (300 MHz, $CDCl_3$) δ 1.7−1.9 (m, 8H, $CH_2CH_2CH_2$), 2.15−2.3 (m, 4H, $CH_2CH_2CH_2$), 2.4−2.6 (m, 8H, $CH_2CH_2CH_2$), 2.65−2.80 (m, 4H, $CH_2CH_2CH_2$), 3.21 (d, J = 12.8 Hz, 4H, CH_2COCH_2), 3.60 (d, J = 12.8 Hz, 4H, CH_2COCH_2), 5.94 (s, 4H, ArH), 6.39 (dd, J = 7.6, 1.5 Hz, 4H, ArH), 6.48 (dd, J = 7.6, 1.5 Hz, 4H, ArH); ^{13}C NMR (75 MHz) δ 28.1, 32.5, 35.5, 49.1, 127.2, 129.7, 131.9, 136.4, 138.1, 207.7; HRMS (FAB) m/z calcd for $C_{42}H_{44}O_2$ 580.3341 [M^+], found 580.3341. Anal. Calcd for $C_{42}H_{44}O_2$: C, 86.85; H, 7.64. Found: C, 86.58; H, 7.68.

Four-Layered [3.3]Paracyclophanes C_{2h} Isomer 4 and D_2 Isomer 5. A mixture of C_{2h} isomer **10** (153 mg, 0.264 mol), 98% $NH_2NH_2\cdot H_2O$ (3 mL), $NH_2NH_2\cdot 2HCl$ (600 mg), KOH (2.6 g), and diethylene glycol (55 mL) was heated at 130 °C for 6 h and then at 200 °C for 5 h with stirring. After cooling, the mixture was poured into ice−water, acidified with concentrated HCl, and extracted with CH_2Cl_2. The CH_2Cl_2 solution was washed with brine, dried with $MgSO_4$, and concentrated to dryness. Purification of the residue by silica gel column chromatography with benzene/hexane (5:4, R_f 0.86) gave **4** (105 mg, 72%) as white crystals. **4**: colorless plates (benzene), mp 295 °C dec; ^{1}H NMR (300 MHz, $CDCl_3$) δ 1.6−1.95 (m, 12H, $CH_2CH_2CH_2$), 2.15−2.80 (m, 24H, $CH_2CH_2CH_2$), 5.72 (s, 4H, ArH), 6.35 (dd, J = 7.6, 1.5 Hz, 4H, ArH), 6.48 (dd, J = 7.6, 1.5 Hz, 4H, ArH); ^{13}C NMR (75 MHz) δ 27.9, 28.9, 32.8, 35.9, 127.0, 129.3, 132.7, 134.6, 134.9, 138.1; HRMS (FAB) m/z calcd for $C_{42}H_{48}$ 552.3756 [M^+], found 552.3754. Anal. Calcd for $C_{42}H_{48}$: C, 91.25; H, 8.75. Found: C, 90.92; H, 8.71.

A mixture of D_2 isomer **11** (72 mg, 0.125 mol), 98% $NH_2NH_2\cdot H_2O$ (4 mL), $NH_2NH_2\cdot 2HCl$ (320 mg), KOH (1.3 g), and diethylene glycol (50 mL) was heated at 130 °C for 18 h and then at 200 °C for 6 h with stirring. After cooling, the mixture was poured into ice−water, acidified with concentrated HCl, and extracted with CH_2Cl_2. The CH_2Cl_2 solution was washed with brine, dried with $MgSO_4$, and concentrated to dryness. Purification of the residue by silica gel column chromatography with benzene/hexane (5:4, R_f 0.86) gave **5** (16 mg, 23%) as white crystals. **5**: Colorless plates (benzene), mp 257 °C dec; ^{1}H NMR (300 MHz, $CDCl_3$) δ 1.6−1.9 (m, 12H, $CH_2CH_2CH_2$), 2.05−2.75 (m, 24H, $CH_2CH_2CH_2$), 5.77 (s, 4H, ArH), 6.36 (dd, J = 7.8, 1.8 Hz, 4H, ArH), 6.49 (dd, J = 7.8, 1.7 Hz, 4H, ArH); ^{13}C NMR (75 MHz) δ 27.5, 28.6, 32.7, 35.8, 126.9, 129.3, 130.9, 134.6, 134.7, 138.0; HRMS (FAB) m/z calcd for $C_{42}H_{48}$ 552.3756 [M^+], found 552.3735. Anal. Calcd for $C_{42}H_{48}$: C, 91.25; H, 8.75. Found: C, 91.06; H, 8.75.

X-ray Crystallographic Study. Measurements were made by using graphite-monochromated Mo Kα (λ = 0.71069 Å; **3**, **4**, **8**, and **10**) or Cu Kα (λ = 1.54187 Å; **1**) radiation and a rotating anode generator. The crystal structures were solved by direct methods [SIR92][30] (**3**), [SIR97][31] (**1**, **8**, and **10**), and [SHELX97][32] (**4**), and refined by the full-matrix least-squares methods. The non-hydrogen atoms were refined anisotropically and hydrogen atoms were refined isotropically. The computations were performed wth the teXan package[33] (**3**, **8**, and **10**) or the Crystalstructure[34] (**1** and **4**). Crystallographic data for the structural analyses of **1**, **3**, **4**, **8**, and **10** have been deposited within the Cambridge Crystallographic Data Centre (CCDC) as 666229, 665070, 665072, 665071, and 665073, respectively. Copies of this information may be obtained from The Director, CCDC, 12 Union Road, Cambridge, CB2 1EZ, U.K. (fax +44 1223 336 033; e-mail deposit@ccdc.cam.ac.uk; or http://www.ccdc.cam.ac.uk/deposit).

Acknowledgement. We are indebted to Professor Takahiko Inazu for his helpful suggestions. We gratefully acknowledge the financial support by a Theme Project of Molecular Architecture of Organic Compounds for Functional Design (Professor Tahsin J. Chow), Institute of Chemistry, Academia Sinica, Taiwan, ROC. We are also grateful for the financial support from a Grant-in-Aid for Scientific Research (B) (No. 18350025) from the Ministry of Education, Culture, Sports, Science and Technology, Japan.

Supporting Information Available: Synthetic procedure for **12** and **13**; summary of crystallographic data and refinement details for **1**, **3**, **4**, **8**, and **10**; ^{1}H and ^{13}C NMR spectra of all new compounds; charge-transfer absorption bands of multilayered [3.3]PCP-diones, three-layered [3.3]PCP **3** and four-layered [3.3]PCP **4**, and two-layered [3.3]PCPs in $CHCl_3$; computational results; cyclic voltammograms of **1**, **2**, **8**, **10,** and **11**; and electronic spectra of **4** and **10** in THF. This material is available free of charge via the Internet at http://pubs.acs.org.

JO8003309

(30) Altomare, A.; Burla, M. C.; Camalli, M.; Cascarano, M.; Giacovazzo, C.; Guagliardi, A.; Polidori, G. *J. Appl. Crystallogr.* **1994**, *27*, 435.
(31) Altomare, A.; Burla, M. C.; Camalli, M.; Cascarano, G. L.; Giacovazzo, C.; Guagliardi, A.; Moliterni, A. G. G.; Polidori, G.; Spagna, R. *J. Appl. Crystallogr.* **1999**, *32*, 115–119.
(32) Sheldrick, G. M. *SHELX-97*, Program for the Refinement of Crystal Structures; University of Goettingen: Goettingen, Germany, 1997.
(33) Crystal Structure Analysis Package; Molecular Structure Corporation, 1985 and 1999.
(34) CrystalStructure 3.8, Crystal Structure Analysis Package; Rigaku and Rigaku/MSC, 2000−2006.